Influence of La_2O_3 promoter on the structure of MnO_x/SiO_2 catalysts

Radu Craciun [a,b,*] and Nicu Dulamita [b]

[a] *Department of Chemistry, Michigan State University, East Lansing, MI48824, USA*
E-mail: craciunr@cemvax.cem.msu.edu
[b] *Technology Department, Faculty of Chemistry and Chemical Engineering, "Babes-Bolyai" University, Cluj-Napoca 3400, Romania*

Received 26 March 1997; accepted 12 May 1997

X-ray diffraction (XRD) and X-ray photoelectron spectroscopy (XPS) analyses have been used to characterize the structure of a La_2O_3-promoted MnO_x/SiO_2 catalyst, before and after its utilization in the oxidative dehydrogenation of ethylbenzene (EB). MnO_x/SiO_2 and $MnO_x/La_2O_3/SiO_2$ catalysts were prepared by pore volume impregnation, using aqueous solutions of (i) La^{3+}-nitrate at an atomic ratio of $La/Si = 0.08$, and (ii) Mn^{2+}-nitrate at an atomic ratio of $Mn/Si = 0.10$, followed by drying and calcination at 500°C in air. XRD data show no diffraction patterns specific to MnO_x on the La_2O_3-promoted MnO_x/SiO_2 catalyst, after calcination. Thus, the presence of La_2O_3 apparently favors the dispersion of manganese oxides during calcination, presumably by forming mixed Mn–La oxides. On the fresh promoted and unpromoted catalysts, after calcination, XRD and XPS analyses indicated that Mn was present mostly as MnO_2 and Mn_2O_3. In the used catalyst, Mn from the unpromoted catalyst degenerated from Mn^{4+} to Mn^{2+}, resulting in formation of Mn_3O_4 species, whereas in the case of La_2O_3-promoted catalyst Mn remained well dispersed as MnO_2 and Mn_2O_3. It appears that La_2O_3 precludes the formation of Mn_3O_4 during the EB dehydrogenation, conserving Mn structure and oxidation state.

Keywords: $La_2O_3/MnO_x/SiO_2$ and MnO_x/SiO_2 catalysts, ethylbenzene dehydrogenation, XRD, XPS, deactivation

1. Introduction

Supported MnO_x and rare earth oxide catalysts have been successfully utilized in oxidative dehydrogenation reactions [1–4]. Previous studies on structural characterization and activity measurements of MnO_x have emphasized catalysts in which γ-Al_2O_3 was used as support [5–9]. The activity of transition metal oxide catalysts can be modified by addition of lanthanide oxides which can act as textural and/or structural promoters [10–15]. Previous studies have shown that rare earth oxide promoted MnO_x/γ-Al_2O_3 catalysts behave as materials with high oxygen storage capabilities, showing excellent catalytic activity in oxidation reactions [8,13–19]. Lanthanum oxide (La_2O_3) is known to be effective as a promoter by increasing thermal resistance (inhibits the loss of the support surface area), dispersion, and the stability of the transition metals used as active catalyst components [11–15]. The structure of La_2O_3-promoted MnO_x/SiO_2 catalysts is strongly dependent on preparation method, the chemical nature of precursors used, and Mn/La ratio and loading [7–17,20].

The purpose of this communication is to examine the influence of La_2O_3 promoter on the structure of MnO_x/SiO_2 catalysts, before and after utilization in the oxidative dehydrogenation reaction of ethylbenzene (EB). Catalytic activity and selectivity at different temperatures will be summarized and presented in correlation with the catalyst structure. X-ray diffraction (XRD) and X-ray photoelectron spectroscopy (XPS) analyses were used to obtain information about the bulk and surface structure, and to characterize the fresh and used, unpromoted and La_2O_3-promoted MnO_x/SiO_2 catalysts.

2. Experimental

Catalysts preparation. The support was prepared using silica-gel material (Davison Chemical Co.), finely ground (< 230 mesh) and calcined in air at 500°C for 24 h, prior to impregnation (surface area = 300 m^2/g). Catalysts derived from lanthanum nitrate used $La(NO_3)_3$ (Aldrich) as precursor whereas those from manganese nitrate used $Mn(NO_3)_2 \cdot 6H_2O$ (Aldrich). The lanthanum and manganese content, calculated relative to silica support, was chosen to be $La/Si = 0.08$ for lanthanum and $Mn/Si = 0.10$, atomic ratio. The catalysts prepared for this study were obtained by incipient wetness impregnation with water-borne precursor solutions. The La_2O_3-promoted MnO_x/SiO_2 catalyst was prepared by sequential impregnation (first lanthanum followed by manganese). All samples were dried at 125°C and calcined for 16 h in air at 500°C after each impregnation step, prior to using them in the EB oxidative dehydrogenation process.

X-ray diffraction (XRD). X-ray powder diffraction patterns were obtained with a Rigaku XRD diffractometer employing Cu Kα radiation ($\lambda = 1.541838$ Å)

* To whom correspondence should be addressed.

and operated at 45 kV and 100 mA. Diffraction patterns were obtained using a scan rate of 1 deg/min with 1/2 mm slits. Powdered samples were mounted on glass slides by pressing the powder into an indentation on one side of the slide.

X-ray photoelectron spectroscopy (XPS). XPS data were obtained using a Perkin-Elmer Surface Science instrument equipped with a magnesium anode (1253.6 eV) operated at 300 W (15 kV, 20 mA) and a 10-360 hemispherical analyzer operated with a pass energy of 50 eV. Spectra were collected using a PC137 board interfaced to a Zeos 386SX computer. The instrument typically operates at pressures below 1×10^{-8} Torr in the analysis chamber. Samples were analyzed as powders dusted onto double-sided sticky tape. Binding energies for the catalyst samples were referenced to the Si_{2p} peak (103.4 eV). XPS binding energies were measured with a precision of ± 0.2 eV or better.

Activity measurements. Oxidative dehydrogenation of ethylbenzene (EB) to styrene was used as a probe reaction for catalysts testing. The reaction was performed in a vertical, fixed-bed quartz reactor equipped with a heating system capable of controlling the temperature with ± 1°C accuracy. The reaction was run at five different temperatures (400, 425, 450, 475, and 500°C), keeping (as much as possible) all the other conditions constant (EB flow rate = 0.13 ml/min, air flow rate = 4.2 ml/min, atmospheric pressure, residence time = 20 s). Typically, products are collected for 30 min during steady-state operation of the reactor. The reaction products exit the bottom of the reactor and are condensed in a cooling flask using an ice-bath. The volume of the liquid product and the flow rate of the gas product are measured during operation in order to conduct a mass balance. The outlet of the reactor was connected to a Riken infrared CO_2 gas analyzer which measured the amount produced in the reaction. Product analyses were performed using a Perkin Elmer 8500 gas chromatograph equipped with FID detector and a Supelco packed column (GP 5% SP-1200/1.75% bentone 34 on 100/120 supelcoport). A good reproducibility of EB, toluene, benzene, and styrene analysis was achieved by direct injection into the column of 1 μl condensed product solution mixed with *n*-pentane as an internal standard (99.9%). A response factor was determined for each component observed in the product mixture (EB, styrene, toluene and benzene). EB conversions and selectivities were reported as average of three consecutive tests in weight% of the EB converted in the reaction. A good carbon recovery was obtained (95–105%).

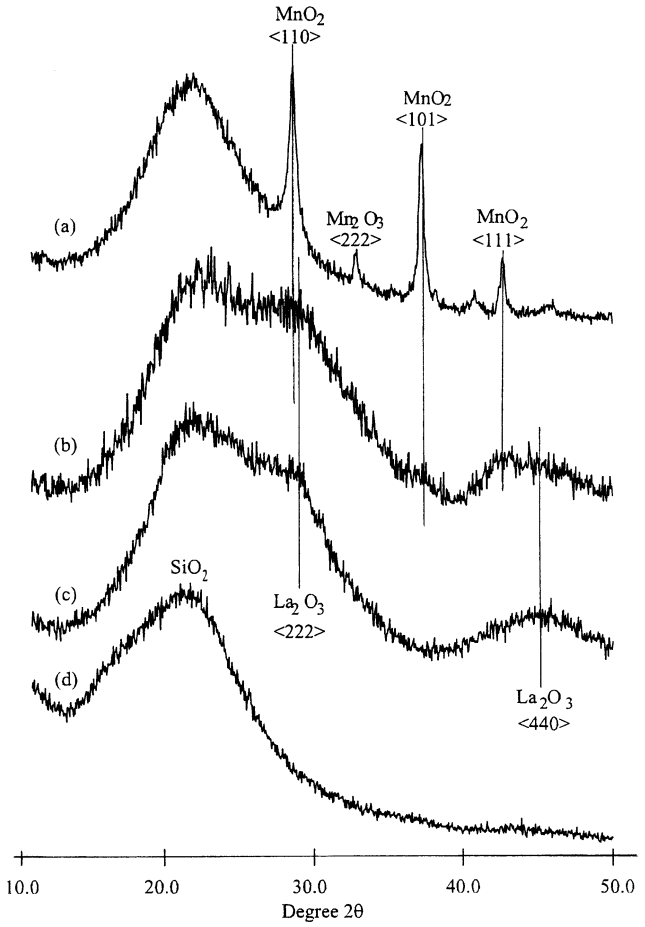

Figure 1. XRD diffraction patterns for the fresh catalysts calcined at 500°C: (a) MnO_x/SiO_2; (b) $MnO_2/La_2O_3/SiO_2$; (c) La_2O_3/SiO_2; (d) SiO_2.

3. Results and discussion

3.1. Fresh catalysts

Figure 1 shows the diffraction patterns for (a) MnO_x/SiO_2, (b) $MnO_x/La_2O_3/SiO_2$, and (c) La_2O_3/SiO_2 catalysts, together with (d) the SiO_2 support for comparison. As assigned in figure 1a, diffraction patterns specific to MnO_2 and Mn_2O_3 were observed [21]. Calcination of the catalyst to 500°C in air led to the formation of a mixed MnO_2–Mn_2O_3 phase on the SiO_2 support. On the La_2O_3-promoted MnO_x/SiO_2 catalyst, only diffuse diffraction patterns specific to the manganese oxides and La_2O_3 species (figure 1b) are observable. This can be attributed to the formation of small particles of mixed Mn–La oxide during calcination. Similarly, in the case of the La_2O_3/SiO_2 catalyst (figure 1c), only diffuse patterns specific to La_2O_3 $\langle 222 \rangle$ and $\langle 440 \rangle$ are observable [21]. This suggests that after calcination of the dried catalyst, small La_2O_3 crystallites are formed on the silica surface. This observation is consistent with the literature data which reported a good lanthanum oxide dispersion on high surface area supports [4,7,13]. In addition to the XRD data presented above, the binding energy values from La_{3d} XPS spectra obtained for both promoted catalysts (for La_{3d} BE = 835.1 eV and BE = 818.3 V correspond to $La_{3d_{5/2}}$ and $La_{3d_{3/2}}$ [15,20]),

also indicate that lanthanum is present on the surface as La_2O_3.

Figure 2 shows the Mn_{2p} XPS spectra in standard MnO_2 (figure 2a) and Mn_2O_3 (figure 2d) species in comparison with the Mn_{2p} spectra in the La_2O_3-promoted used (figure 2b) and fresh (figure 2c) and in the unpromoted MnO_x/SiO_2 used (figure 2e) and fresh (figure 2f) catalysts, respectively. The low S/N observed for the Mn_{2p} XPS spectra is due to short acquisition time, which avoids X-ray photoreduction of manganese during analysis [22]. For the fresh promoted catalyst (figure 2c), the Mn_{2p} signal indicates the presence on the catalyst surface of manganese with higher oxidation state, probably Mn^{4+} which has BE = 642.0 eV, close to the BE observed in Mn_{2p} (figure 2a) from MnO_2 [23–25]. In the case of the fresh unpromoted catalyst (figure 2f), the Mn_{2p} XPS spectrum shows that manganese is present as mixed Mn^{3+}/Mn^{4+} with a profile similar to a mixed Mn_{2p} spectrum from MnO_2 (figure 2a) and Mn_2O_3 (figure 2d). However, the peak is shifted toward the BE of Mn^{4+} species (642.0 eV), indicating a higher MnO_2 content. This observation is in good agreement with the XRD data (figure 1a) which show diffraction patterns specific to both MnO_2 and Mn_2O_3 species, at ratio $r = 0.89$, where $r = A_{(\langle 110\rangle MnO_2)}/(A_{(\langle 110\rangle MnO_2)} + A_{(\langle 222\rangle Mn_2O_3)})$.

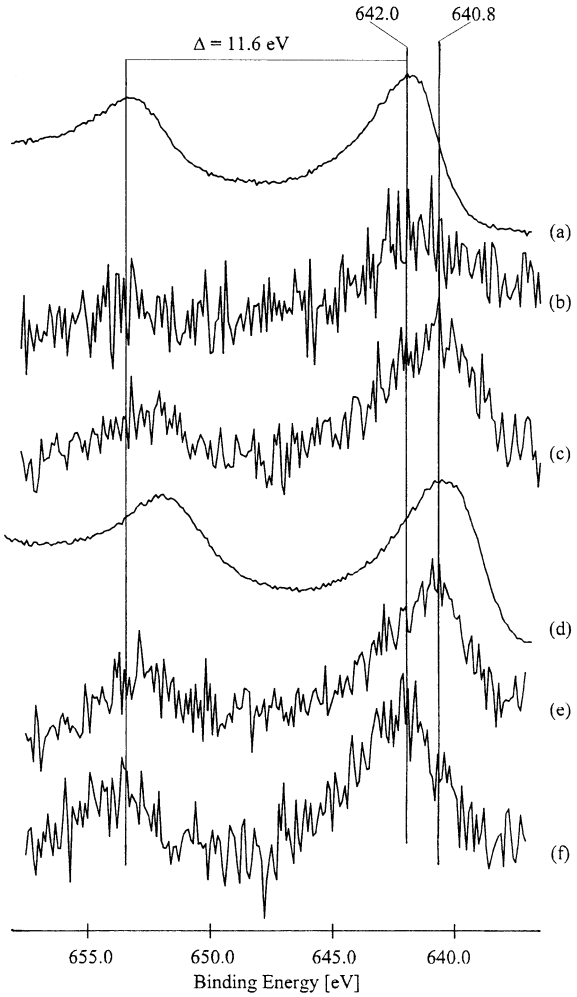

Figure 2. Mn_{2p} XPS spectra of (a) MnO_2, (b) used and (c) fresh $MnO_2/La_2O_3/SiO_2$ catalysts in comparison with (d) Mn_2O_3, (e) used and (f) fresh MnO_2/SiO_2 catalysts.

3.2. Catalyst activity

Figure 3 shows the variation of ethylbenzene conversion with temperature (400–500°C range), for the unpromoted and La_2O_3-promoted MnO_x/SiO_2 and SiO_2 catalysts. Table 1 shows selectivity data for EB dehydrogenation to styrene, total oxidation to CO_2 and cracking to toluene and benzene, the main chemical processes observed in this study. GC analysis of the gas product collected during the catalytic oxidation of EB identified, beside CO_2, other gas components such as CH_4, C_2H_4 and CO. At 400°C the La_2O_3-promoted MnO_x/SiO_2 catalyst shows the highest conversion (23.1%) compared with the other catalysts for which conversion reaches only 10–14%. The highest selectivity toward styrene formation is shown by MnO_x/SiO_2 (77.5%) but at very low conversion (13.2%). This catalytic activity can be correlated with the capability of MnO_2 from the SiO_2 support to act as an oxygen donor during the oxidative dehydrogenation process and form H_2O. In all cases, the La_2O_3-promoted MnO_x/SiO_2 catalyst shows a higher selectivity toward toluene formation ($\sim$ 10%), a partial oxidation process, a lower selectivity toward styrene (5–10% less), and a lower conversion ($\sim$ 5%), in comparison with the unpromoted MnO_x/SiO_2 catalyst. Considering both conversion and selectivity toward styrene, La_2O_3-promoted MnO_x/SiO_2 catalyst seems to be a good catalyst in the oxidative dehydrogenation of ethylbenzene, with selectivity up to 65.6% and conversion of 23.1%, at low temperature (see table 1). As expected, for each catalyst the EB conversion increased with temperature, reaching $80 \pm 3\%$ at 500°C. The variation in selectivity data observed for each catalyst shows a similar trend at 400

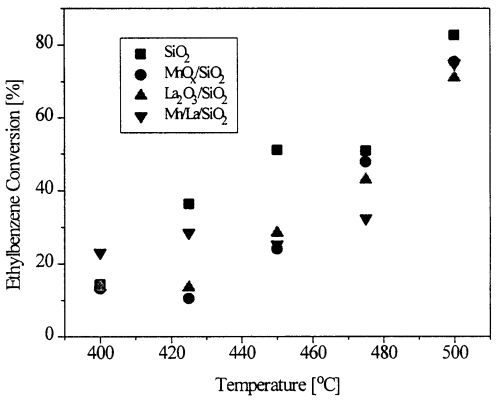

Figure 3. Conversion data from ethylbenzene oxidative dehydrogenation reaction.

Table 1
Selectivity data from ethylbenzene oxidative dehydrogenation reaction

Catalyst	Selectivity (%)											
	styrene			benzene			toluene			CO_2		
	425°C	475°C	500°C	425°C	475°C	500°C	425°C	475°C	500°C	425°C	475°C	500°C
SiO_2	42.3	43.8	32.4	24.4	38.0	56.1	17.1	12.7	8.5	6.5	3.5	2.1
MnO_x/SiO_2	77.5	52.7	41.8	14.3	34.8	41.2	12.5	17.2	12.9	3.2	0.0	2.3
La_2O_3/SiO_2	60.4	45.1	37.9	5.0	34.0	38.9	5.7	13.5	22.5	23.4	7.1	3.4
$Mn/La/SiO_2$	65.6	46.2	37.2	16.6	33.0	39.7	12.0	27.2	22.8	6.3	0.0	3.8

and 450°C (not shown) as those found at the temperatures reported in table 1. As observed from the data presented in table 1, pure SiO_2 support acts as a cracking catalyst, favoring benzene (56.1%) rather than styrene (32.4%) formation. This catalytic activity can be attributed to the surface acid groups present on the high surface area SiO_2 support (mostly Brønsted acid sites [3,20]) which will act as active sites for cracking reactions [26]. La_2O_3 is known to have the capability to disperse well on high surface area supports [13,15,20], so the surface acid groups present on the SiO_2 will be deactivated. As a consequence, in the case of the La_2O_3/SiO_2 catalyst the EB conversion and selectivity toward benzene formation are very low (see table 1 and figure 3), but the catalyst is still selective toward styrene formation (60.4%).

3.3. Used catalyst

The used catalysts from EB oxidative dehydrogenation reaction were analyzed by XRD and XPS. Diffraction patterns obtained for these catalysts are presented in figure 4. In the case of the MnO_x/SiO_2 catalyst, new patterns are observable (figure 4a), identified based on literature data and analysis of reference compounds, and thus, attributed to Mn_3O_4 ($MnO{\cdot}Mn_2O_3$) species formed during the catalytic process. In the oxidation reaction, manganese oxide species act as oxygen donors. On the used catalyst, MnO_2 can be regenerated by recalcination at 500°C in air. The XRD spectra of used La_2O_3-promoted MnO_x/SiO_2 and SiO_2 catalysts (figures 4b and 4c) remain unchanged in comparison with the fresh ones (figures 1b and 1c). The presence of La_2O_3 seems to affect the resistance of MnO_2 to reduction during the catalytic process. These observations are in agreement with previous studies which have shown that La_2O_3 promoter can play an important role in oxygen mobility on oxidation catalysts [27]. Also it was found that that the presence of La_2O_3 influences the dispersion and resistance to oxidation state changes in catalytic systems containing Rh [10], Ce [11], or Co [13,15].

Mn_{2p} XPS spectra for used La_2O_3-promoted MnO_x/SiO_2 catalyst, presented in figure 2b, show a weak signal with the major peak located at BE = 642.0 eV corresponding to Mn^{4+} [22–25]. Shifts toward higher BE reported in the literature were correlated to highly dispersed surface manganese oxide on the support [24,25]. The BE of Mn_{2p} is higher for the dispersed phase than for the bulk manganese oxide, reflecting the interaction of Mn with lanthanum or silica [24]. This observation comes in addition to the previous data obtained from XRD, which show the absence of any clear diffraction pattern for MnO_x on lanthanum-promoted SiO_2 catalyst. Due to the low S/N of the Mn_{2p} XPS spectrum for the used La_2O_3-promoted MnO_x/SiO_2 catalyst, the presence of Mn_2O_3 can be ruled out. In addition, no significant shift in BE for La_{3d} was observed for the used

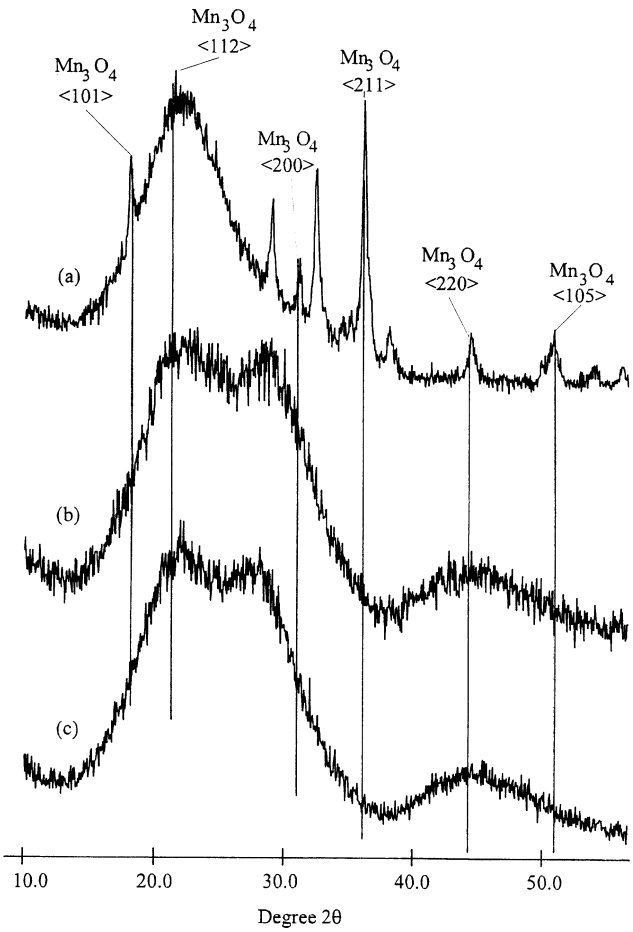

Figure 4. XRD diffraction pattern of used: (a) MnO_2/SiO_2; (b) $MnO_2/La_2O_3/SiO_2$; (c) La_2O_3/SiO_2 catalysts.

catalyst compared with the fresh La_2O_3-promoted MnO_x/SiO_2 catalyst, which can indicate the transformation of La_2O_3 into a perovskite-type $MnLaO_x$ structure (the shift in BE should be larger than 1.5 eV [15]).

For the unpromoted used MnO_x/SiO_2 catalyst (figure 2e), the BE shifts to 640.8 eV, corresponding to manganese with lower oxidation states of Mn^{2+} or Mn^{3+} [22–25]. It is hard to identify a signal specific to Mn^{2+} species, due to the overlap in BE values with Mn^{3+} species. Literature data show Mn_{2p} binding energy values for Mn_3O_4 species in the 641.3–641.4 eV range, and for Mn_2O_3 species in the 641.3–641.9 eV range [24]. The presence of manganese at low oxidation states on the used catalyst, is consistent with the observation of XRD diffraction patterns specific to Mn_3O_4 species formed on the unpromoted MnO_x/SiO_2 catalyst.

Other interesting changes were observed in the C_{1s} XPS spectra of the used catalysts, presented in figure 5. On the La_2O_3-promoted MnO_x/SiO_2 catalyst (figure 5a), three C_{1s} peaks, C_0 at BE = 284.2 eV, C_1 at BE = 285.4 eV, and C_3 at BE = 290.8 eV, were observed. A C_2 peak (BE $\approx$ 287 eV) is not clearly observed. Each carbon peak can be attributed to different types of carbon [28]. Briefly, C_0 corresponds to graphitic type of carbon, C_1 to hydrocarbon material, C_2 to a carbon single-bonded to an oxygen, and C_3 to a carbon double-bonded to oxygen (carbonyl or carboxyl groups). There are two clear new features in the C_{1s} XPS spectrum of the used La_2O_3-promoted MnO_x/SiO_2 catalyst: (i) the intense C_0 peak corresponding to carbon black material deposited on the catalyst surface during its use in the EB oxidation; (ii) the presence of a C_3 peak corresponding to some oxygenated hydrocarbon material which remained deposited on the catalyst surface. Both peaks can be related to the strong catalytic oxidation activity of the La_2O_3-promoted catalyst. In comparison, on the used MnO_x/SiO_2 (figure 5b) and La_2O_3/SiO_2 (figure 5c) catalysts, XPS could detect only carbon specific to hydrocarbon residue, commonly present on any surface (C_1 peak at BE = 285.4 eV) [22,25]. There were no significant changes in the La_{3d} and O_{1s} XPS spectra for the used catalysts in comparison with the fresh catalysts.

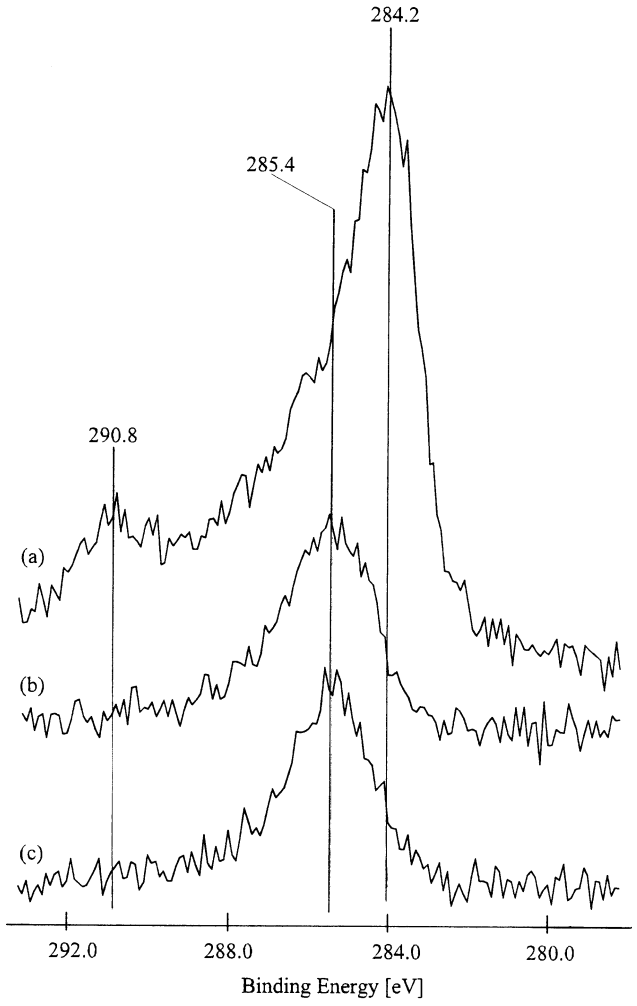

Figure 5. C_{1s} XPS spectra for used: (a) $MnO_2/La_2O_3/SiO_2$; (b) MnO_2/SiO_2; (c) La_2O_3/SiO_2 catalysts.

4. Conclusions

On the fresh catalyst, XRD and XPS analysis of the unpromoted catalyst indicated that manganese was present mostly as MnO_2 and Mn_2O_3. The presence of La_2O_3 favors the dispersion of manganese oxides deposited on SiO_2 catalyst during calcination by forming mixed Mn–La oxides (no diffraction pattern specific to MnO_x observed). However, further investigations using Raman or EPR spectroscopy are necessary to obtain additional information about the exact nature of the mixed Mn–La oxide formed. Used in the oxidative dehydrogenation of EB, at low temperature (425°C), unpromoted and La_2O_3-promoted MnO_x/SiO_2 catalysts act selectively toward styrene formation at low EB conversion. At high temperature (500°C), EB conversion increases but the selectivity toward styrene decreases. Analysis of the used catalysts showed that the manganese oxidation state on unpromoted catalysts degenerates from Mn^{4+} to Mn^{2+}, leading to the formation of Mn_3O_4 species. On the La_2O_3-promoted MnO_x/SiO_2 catalyst, manganese remains dispersed with a structure similar to that of the fresh catalyst and precludes the formation of Mn_3O_4 (no change in oxidation state observed).

Acknowledgement

The authors are grateful for the assistance of Dr. Ned Jackson and Dr. Simon Garrett from Department of Chemistry and Dr. Dennis Miller from Chemical Engineering Department at Michigan State University.

References

[1] F. Cavani and F. Trifirò, Appl. Catal. 133 (1995) 219.
[2] T. Akiyama, Y. Enomoto and T. Shibamoto, J. Agric. Food Chem. 26 (1978) 1176.
[3] R. Craciun, PhD Thesis dissertation, Michigan State University, East Lansing, USA (1997).
[4] S. Sugiyama, K. Sogabe, T. Miyamoto, H. Hayashi and J.B. Moffat, Catal. Lett. 42 (1996) 127.
[5] J.J. Kim and S.W. Weller, Appl. Catal. 33 (1987) 15.
[6] P.W. Selwood and J. Mooi, J. Am. Chem. Soc. 74 (1952) 2461.
[7] B.R. Strohmeier and J. Hercules, J. Phys. Chem. 88 (1984) 4922.
[8] M.A. Baltanas, A.B. Stiles and J.R. Katzer, Appl. Catal. 28 (1986) 13.
[9] F. Kapteijn, L. Singoredjo, M. van Driel, A. Andreini, J.A. Moulijn, G. Ramis and G. Busca, J. Catal. 150 (1994) 105.
[10] R. Kieffer, A. Kiennemann, M. Rodriguez, S. Bernal and J.M. Rodriguez-Izquirdo, Appl. Catal. 42 (1988) 77.
[11] R.K. Usmen, G.W. Graham, W.L.H. Watkins and R.W. McCabe, Catal. Lett. 30 (1995) 53.
[12] Y. Jun-Ying and W.E. Swartz Jr., Spectrosc. Lett. 17 (1984) 331.
[13] J.S. Ledford, M. Houalla, A. Proctor and D.M. Hercules, J. Phys. Chem. 93 (1989) 6770.
[14] M. Shelef, L.P. Haack, R.E. Soltis, J.E. DeVries and E.M. Logothetis, J. Catal. 137 (1992) 114.
[15] J.S. Ledford, Y.M. Kim, M. Houalla, A. Proctor and D.M. Hercules, Analyst 117 (1992) 323.
[16] T. Yamashita and A. Vannice, J. Catal. 163 (1996) 158.
[17] S. Imamura, M. Shono, N. Okamoto, A. Hamada and S. Ishida, Appl. Catal. 142 (1996) 279.
[18] A.S. Ivanova, V.A. Dzisco, E.M. Moroz and S.P. Nosckova, Kinet. Katal. 27 (1986) 285.
[19] M.A. Baltanas, S.J. DeCanio, J.R. Katzer and C. Dybowski, Acta Chim. Hung. 118 (1986) 285.
[20] R. Craciun and N. Dulamita, Progr. Catal., submitted (1996).
[21] W.F. McClune, *Powder Diffraction File, Inorganic Phases* (International Center for Diffraction Data, Swarthmore, 1983) pp. 279, 599, 730, 731.
[22] J.K. Moulder, W.F. Stickle, P.E. Sobol and K.D. Bomben, *Handbook of X-ray Photoelectron Spectroscopy* (Perkin-Elmer Co., Eden Prairie, 1992) pp. 40–87.
[23] E. Paparazzo, G.M. Ingo and N.J. Zacchetti, J. Vac. Sci. Technol. A 9 (1991) 1416.
[24] F. Kapteijn, A.D. van Langeveld, J.A. Moulijn, A. Andreini, M.A. Vuurman, A.M. Turek, J.M. Jehng and I.E. Wachs, J. Catal. 150 (1994) 94.
[25] A. Wollner, F. Lange, H. Schmelz and H. Knözinger, Appl. Catal. A 94 (1993) 181.
[26] B.C. Gates, *Catalytic Chemistry* (Wiley, New York, 1992) p. 276.
[27] M.S. Islam and D.J. Ilett, in: *New Developments in Selective Oxidation II,* eds. V. Cortes Corberan and S. Vic Bellon (Elsevier, Amsterdam, 1994) pp. 427–434.
[28] T.L. Barr, *Modern ESCA: the Principles and Practice of X-ray Photoelectron Spectroscopy* (CRC Press, Boca Raton, 1995).